

OPEN

Nanodiamond phantoms mimicking human liver: perspective to calibration of T1 relaxation time in magnetic resonance imaging

Anna Sękowska¹, Daria Majchrowicz^{2,3}, Agnieszka Sabisz⁴, Mateusz Ficek², Barbara Bułto-Piontecka⁵, Monika Kosowska², Lina Jing⁶, Robert Bogdanowicz² & Małgorzata Szczerska^{2*}

Phantoms of biological tissues are materials that mimic the properties of real tissues. This study shows the development of phantoms with nanodiamond particles for calibration of T1 relaxation time in magnetic resonance imaging. Magnetic resonance imaging (MRI) is a commonly used and non-invasive method of detecting pathological changes inside the human body. Nevertheless, before a new MRI device is approved for use, it is necessary to calibrate it properly and to check its technical parameters. In this article, we present phantoms of tissue with diamond nanoparticles dedicated to magnetic resonance calibration. The method of producing phantoms has been described. As a result of our research, we obtained phantoms that were characterized by the relaxation time T1 the same as the relaxation time of the human tissue T1 = 810.5 ms. Furthermore, the use of diamond nanoparticles in phantoms allowed us to tune the T1 value of the phantoms which open the way to elaborated phantoms of other tissues in the future.

Magnetic resonance imaging (MRI), is a non-invasive technique for creating detailed images of the human body. This method allows for obtaining high-resolution cross-sectional images of tissue in any surfaces. Therefore now is a widely available, powerful instrument for non-invasive imaging of soft tissues better than X-rays, computerized tomography scans or ultrasound¹⁻³. Chronic liver diseases represent an important global health problem.

MRI is a technique which plays a significant role in diagnosis of different liver disorders. The MRI investigation can show and confirm diffuse liver damage due to metabolic diseases or cirrhosis. Furthermore, MRI plays an important role in differentiation in primary hepatic malignancies or metastatic diseases⁴. The parameters characteristic for a sample investigated by the means of MRI are longitudinal relaxation time T1 and transverse relaxation time T2, which directly depend on the biophysical structure of the test substance and the biochemical environment⁵. The study of relaxation times and their dependence on the magnetic field, temperature, pH, etc. provides valuable information on the structure and molecular dynamics of the substance. A significant amount of biological tissue phantoms used for an MRI scanner calibration is created to examine the scanner's technical parameters⁶⁻¹³. Phantoms used to calibrate relaxation times are scarce. The few phantoms dedicated to the calibration of relaxation times are mainly oil based or water based (e.g. aqueous solutions of inorganic acid salts^{12,14-17}). Due to their liquid state, the calibration process is more time-consuming because the liquid must stabilize before the measurement can start. Relaxation agents such as gadolinium trichloride, which were found to enable adjustment of T1 relaxation time, are toxic, therefore their use for biomedical applications is excluded¹⁸.

¹Department of Medical Physics, Pomeranian Medical University, 12 Ku Słońcu Street, 71-080, Szczecin, Poland.

²Department of Metrology and Optoelectronics, Faculty of Electronics, Telecommunications and Informatics, Gdańsk University of Technology, 11/12 Narutowicza Street, 80-233, Gdańsk, Poland. ³SUPA School of Physics and Astronomy, University of St Andrews, North Haugh, KY16 9SS, St, Andrews, UK. ⁴2-nd Department of Radiology, Medical University of Gdansk, 3a Marii Skłodowskiej-Curie Street, 80-210, Gdansk, Poland. ⁵Department of Nephrology, Transplantology and Internal Diseases, Faculty of Medicine, Medical University of Gdańsk, 3a Marii Skłodowskiej-Curie Street, 80-210, Gdansk, Poland. ⁶Department of Radiology, Beijing Tiantan Hospital, Capital Medical University, 119 West Fourth Ring South Road, Fengtai District, 100070, Beijing, China. *email: malszcze@pg.edu.pl

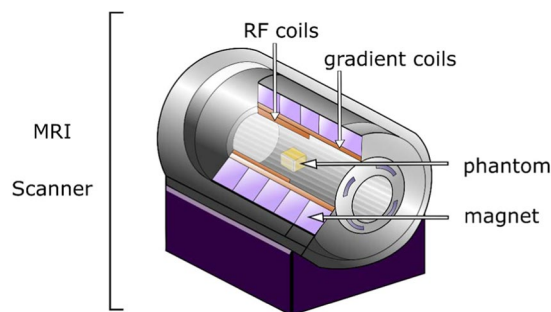


Figure 1. Visualization of the experiment.

In this paper, we report the development and magnetic characteristics of liver phantoms for the calibration of an MRI scanner. They were produced on the basis of agar and carrageen, and diamond nanoparticles. The obtained phantoms with the addition of diamond nanoparticles (size of 4–5 nm) had relaxation time T_1 very similar to the selected human body tissue - liver.

Experimental – Phantom characteristics

The MRI imaging was performed using phantoms containing nanodiamond particles fabricated by detonation method (DND) and purified by Ray Techniques Ltd. (Israel). The utilized nanodiamond particles have hydroxyl-terminated surface revealing hydrophilic nature as pointed out by Ray Techniques Ltd. (RT-DND-L). The RT-DND particles are monocrystalline, poly-dispersed with average size of 4–5 nm. The dimethyl sulfoxide (DMSO) was applied here as a dispersant of RT-DND particles in agreement with deagglomeration procedures and DND-DMSO interactions reported by Shenderova *et al.*^{19,20}.

The RT-DND particles were dispersed in DMSO using ultrasound Bandelin Sonopuls HD 2200 sonicator (Berlin, Germany), working in a pulse mode to avoid overheating of the liquids²¹. The suspension was prepared by 5-min-long high-power ultrasound sonication which disintegrates partially the ND aggregates, allowing for marginal effect on surface modification. The 0.1 wt.% RT-DND concentration in DMSO was applied. The process resulted in colloiddally stable suspension with average aggregate size of 70–80 nm, being in agreement with previous data shown by Shenderova *et al.*¹⁹. The particle sizes were measured with dynamic light scattering (DLS) using a Malvern Zetasizer Nano ZS instrument (UK). The content of RT-DND:DMSO suspension in prepared phantoms DNP-0, DNP-8, DNP-10, DNP-12 was set to 0%, 8%, 10% and 12%, respectively.

Due to the fact that the prepared phantoms are to be used in calibration of magnetic resonance scanner (Fig. 1), two types of measurements were carried out: T_1 and T_2 relaxation time measurements. T_1 measurement was performed in order to verify whether nanodiamond particles can be used as T_1 modifiers in MRI phantoms. T_2 measurement was carried out to check the nanodiamonds influence on obtained T_2 values.

The first type of measurement was the measurement of relaxation time T_1 using the Inversion Recovery method. A series of scans was obtained for four different inversion times TI: 200, 400, 800, 1200 [ms], at four different depths. 20 measurements were taken for each sample from a given group (5 on each of 4 scans). Based on the acquired scans T_1 -maps for each slice were obtained with the use of MRmap program (Mountain Rescue, UK). Moreover, the investigated phantoms were measured with the use of a multi-echo spin-echo sequence. A series of phantom scans for six moments of time 1 TE (13 ms), 2TE, 4TE, 5TE, and 6TE on ten different depth levels was obtained. The maps of relaxation time T_2 for each slice were achieved by the means of RadiAnt software (Medixant, Poland). For the obtained maps, measurements of relaxation time T_2 were carried out at different phantom depths, each time five measurement areas located centrally on one phantom layer were tested. For each phantom, 25 measurements were taken. MRI imaging was performed at the Gdansk University of Medicine by the trained medical physics, supervised by Medical Doctor of Radiology.

Result

The first type of measurement, which was made for phantoms with the addition of detonation nanodiamonds and DMSO, was the measurement of relaxation time T_1 using the Inversion Recovery method. Exemplary T_1 -map of phantoms with nanodiamond RT-DND-L suspension and DMSO and T_1 Recovery curve for phantom DNP-8 are presented in Fig. 2.

The results of relaxation time T_1 measurements are presented in Fig. 3. A linear regression curve was adopted (model of linear changes of T_1 relaxation time with the change of suspension content in the phantom) and its coefficient of determination was calculated, $R^2 = 0.9997$.

On the basis of the relaxation time T_1 measurements, we can see that the dependence of relaxation time on the content of nanoparticles is linear. This allows a simple way to make phantoms of specific parameters. The correlation coefficient R^2 is almost equal to one, which indicates that the adopted mathematical model nearly ideally describes the measurement data. The appropriate adjustment of nanodiamond concentration in the examined range will allow production of phantoms reflecting the properties of the liver. Next, the relaxation time T_2 was measured. The obtained results are presented in Fig. 4.

The results of relaxation time T_2 measurements are presented in Fig. 5. The correlation coefficient of the linear fit is equal to $R^2 = 0.8838$.

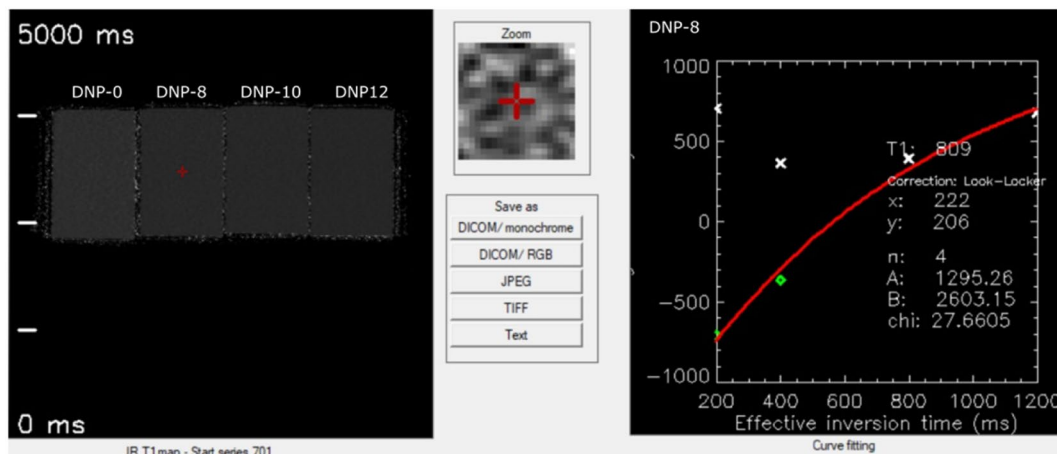


Figure 2. T₁-map of phantoms with nanodiamond RT-DND-L suspension and DMSO and T₁ Recovery curve for phantom DNP-8.

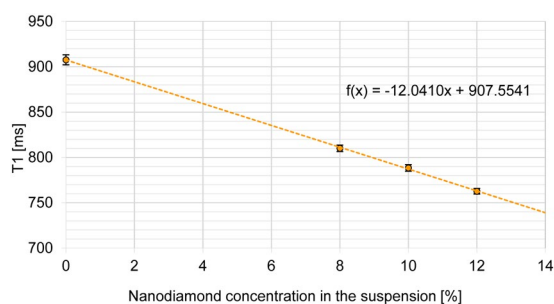


Figure 3. Relaxation time T₁ of the produced phantoms as a function of the nanodiamond concentration in the used suspension.

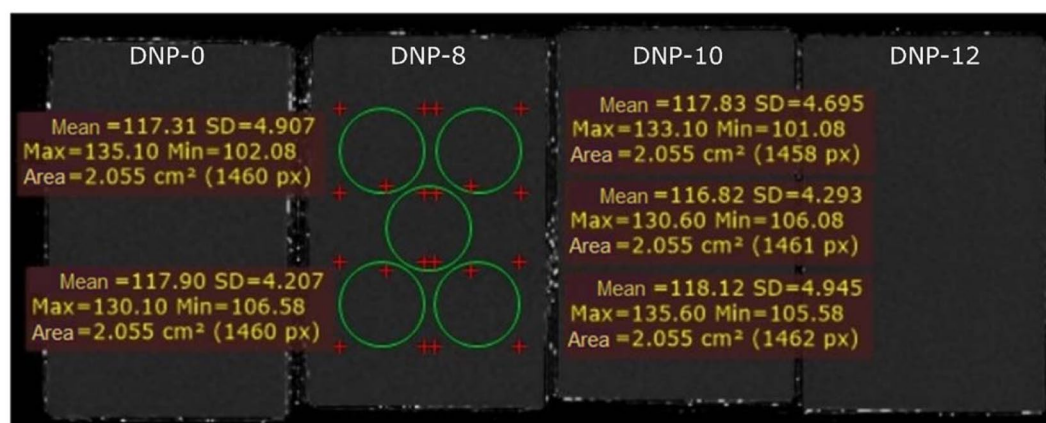


Figure 4. T₂-map of phantoms with nanodiamond RT-DND-L suspension and DMSO, and T₂ measurements for phantom DNP-8.

Phantoms with the addition of nanodiamond suspension provide stable values of T₂, similar to the pure agar-carageen phantom (117.92 ms ~ 118.55 ms). This suggests that the value of relaxation time T₂ can be tuned by proper adjustment of agar content¹⁷. We obtained phantoms which were characterized by the relaxation time T₁ = 810.1 ms the same as the relaxation time of the human liver T₁ liver = 810.5 ms²². The relative error of the relaxation time T₁ of the liver and the produced phantom is 0.049%. The relaxation time T₂ of the studied phantom (117.6 ms) significantly differs from the characteristic value of the liver tissue (38.0 ms). However, an adequate adjustment of the agar concentration will also allow the adjustment of T₂ relaxation time, which is the subject of further research. Taking into consideration obtained result we can say that we elaborated a solid

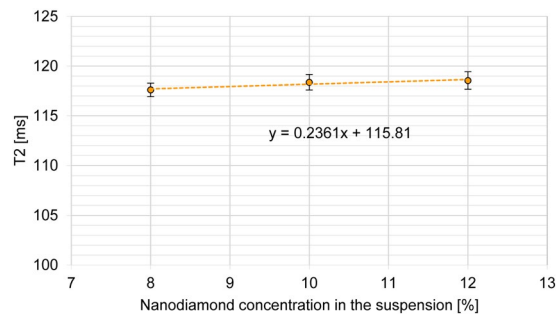


Figure 5. Relaxation time T2 of the produced phantoms as a function of the concentration of the used suspension.

phantom mimicking the human liver specific in terms of its T1 relaxation time. We obtained the value of T1 at the same level as the one reported in the medical database and even though the T2 is not yet properly tailored now, we expect it to be achievable by change of agar content in the phantom.

Discussion

Until now, a few groups have reported production of MRI phantoms. For example, Bazrafshan *et al.* reported a liver polyacrylamide MRI gel phantom mimicking the T1 and T2 of liver up to 75 °C making it possible to be used in thermal therapy²³. However, T1 values measured at different temperatures differ from the tissue values by around 10–15%. Kato *et al.* presented MRI phantoms mimicking times T1 and T2 for desired human tissue with an accuracy of 1 ms¹⁸. The preparation procedure requires many ingredients though, making it relatively complicated. Brzozowski *et al.* proposed MRI phantoms with gellan gum-based gels instead of agar, which were doped with superparamagnetic iron nanoparticles as T2 modifier and either MnCl₂ or GdCl₃ as T1 modifiers²⁴. The presented mathematical model showed the relation between a concentration of contrast agent with adj. R² > 0.97 for longitudinal relaxation rates, and adj. R² > 0.87 for transverse relaxation rates.

The main objective of this study was to present the method for producing phantoms of tissue with the use of nanodiamond particles for calibration of magnetic resonance scanner. We showed the linear relation between the value of T1 and concentration of nanodiamonds allowing production of magnetic phantoms of desired tissue. The goal was achieved and the T1 parameter of our phantom is the same as a T1 value for liver tissue. The changes in T1 with the change of nanodiamond concentration in the used solution is described by correlation coefficient R² = 0.9997 (adj. R² = 0.9996). This gives us the possibility to produce the phantoms of other tissue. The study needs further investigation regarding the tailoring of T2 value. However, it was shown that this parameter remains stable regardless of nanodiamonds content, meaning that T1 modification by nanodiamonds does not affect the T2. One of the basic limitations of the study was the availability of only one MRI scanner with a magnetic field strength of 3.0 T. It would be advisable to study the relaxation times of the prepared phantoms for MRI scanners with different magnetic field strengths in order to verify the results.

Conclusions

While phantoms mimicking selected properties of tissues are used in testing and verifying measurement devices, there is still a lack of the phantoms for magnetic resonance calibration. Therefore, we developed a new group of phantoms utilizing diamond nanoparticles, which are dedicated for MRI calibration. We found that the relaxation time T1 of these phantoms is easily tunable because of the linear relationship between its value and concentration of the nanodiamonds. This unique solution provides a possibility to tailor the T1 parameter to desired value in a simple, cost-effective and fast (few hours) way. Furthermore, the developed phantoms are produced in a gel form. Commonly produced phantoms in a liquid form show many limitations: not only is the time of their use relatively short, but also obtaining the multi-layer systems is impossible. The examination procedure is also unnecessarily prolonged due to the requirement of liquid stabilization. The proposed approach solves the aforementioned problems, while keeping the simplicity of preparation procedure.

In this paper, phantoms for an MRI scanner calibration with nanodiamonds were presented. RT-DND-L detonation nanodiamonds were used during the investigation. Measurements of their magnetic properties were made in order to verify the possibility of their use for the calibration of magnetic resonance scanner. The addition of the suspension did not significantly affect the change in the relaxation time T₂ (this parameter was more stable though) and the dependence of time T1 on the suspension concentration turned out to be linear. The obtained phantoms with the addition of diamond nanoparticles with an average size of 4–5 nm were characterized by the relaxation time T1 which is very similar to the selected tissue of a human body - liver. The addition of the suspension has a significant effect on the change of relaxation times T1 and T2, and the relationship in the case of relaxation time T2 does not show linearity. However, the analysis of the measurements of the relaxation time T2 shows that the addition of suspension affected the change in the measured value to some extent. The proper tailoring of the T2 parameter is the subject of our further investigations.

Quantitative MRI is now one of the top methods in radiology. There are growing number of articles and hence acquisition protocols in clinical studies considering T1 measurements. The use of such phantoms will allow for verification of accuracy of results by different MRI. Such phantom can help to optimise the instrumental precision and support quality control. Due to their solid form, the calibration process will be shortened. In addition, these

phantoms do not contain any toxic compounds in contrast to frequently used T1 modifier - gadolinium chloride. Furthermore, our investigation opens the new possibility to create the solid phantoms of other tissues and organs for MRI calibration in the future, which has started to be a standard in other methods of biological samples imaging like optical imaging^{25,26}.

Methods

Nanodiamond preparation. The method of phantoms production was developed on the basis of the technique using agar media for microbiological tests. The bases of the produced phantoms are agar-carrageen gels. The mechanical properties of the phantoms mainly depend on carrageen, and changes in the relaxation time T2 are dependent on agar. The studies determined that carrageenan concentration should not exceed 2% due to technological difficulties. The composition of the target phantoms for a magnetic resonance scanner calibration was enriched by the addition of nanodiamond suspension. Nanodiamonds were added to the agar-carrageen gel to modify the relaxation time T1. The solution base (the dispersing phase), is dimethyl sulfoxide (DMSO). In this article, the phantoms with the addition of a 0.10% suspension prepared on the basis of RT-DND-L nanodiamond powder (Ray Techniques Ltd Israel) containing 8% to 12% of the nanoparticles with an average size of 4–5 nm were performed.

Phantom fabrication. Distilled water, agar (1.413%) and carrageenan (2%) were used to produce a group of phantoms with nanoparticles of a certain type, differing in the concentration of the suspension. In order to fully distribute the agar and carrageenan, the components were heated to boiling, stirred and put into the autoclave for about 45 minutes, with the inside temperature of 126°C. The gel base of phantoms was poured into the prepared nanodiamond suspensions. The contents of the individual beakers were then thoroughly mixed and subjected to the autoclave. Then the samples were poured into molds and placed under cover to congeal.

MRI setup. Magnetic resonance imaging was performed with the Philips Healthcare Achieva 3.0T-TX using a 32-channel coil dedicated for the examination of the heart. MultiTransmit technology used in this system eliminates dielectric shading by applying simultaneous transmission from multiple RF signal sources, ensuring optimal homogeneity and consistency of the image and faster scanning rate [19]. Measurements of relaxation time T1 were performed using the Inversion Recovery (IR) method. The measurement parameters were as follows: TR pulse repetition time was 1600 ms, TE echo time per 15 ms, TI inversion times: 200, 400, 800, 1200 ms, voxel size $0.9375 \times 0.9375 \times 3$ mm. Measurements of relaxation time T2 were carried out using the multi-echo method using the spin echo technique. The measurement parameters were as follows: the pulse repetition period was set to 2000 ms, TE 13 ms echo time, voxel size $0.75 \times 0.75 \times 2.5$ mm.

Received: 10 July 2019; Accepted: 30 March 2020;

Published online: 15 April 2020

References

1. Chrysikopoulos, H. S., *Clinical MR Imaging and Physics: A Tutorial*, Springer (2009).
2. Grover, V. P. B. *et al.* Magnetic Resonance Imaging: Principles and Techniques: Lessons for Clinicians. *Journal of Clinical and Experimental Hepatology* **5**, 246–255 (2015).
3. Ridgway, J. P. Cardiovascular magnetic resonance physics for clinicians: part I. *Journal of Cardiovascular Magnetic Resonance* **12**, 71 (2010).
4. Chundru, S. *et al.* MRI of diffuse liver disease: characteristics of acute and chronic diseases. *Diagn Interv Radiol* **20**, 200–208 (2014).
5. Tang, X. *et al.* Magnetic resonance imaging relaxation time in Alzheimer's disease. *Brain Research Bulletin* **140**, 176–189 (2018).
6. Feder, I., Duadi, H. & Fixler, D. Experimental system for measuring the full scattering profile of circular phantoms. *Biomed Opt Express* **6**, 2877–2886 (2015).
7. Esenaliev, R. O., Larin, K. V., Larina, I. V. & Motamedi, M. Noninvasive monitoring of glucose concentration with optical coherence tomography. *Opt. Lett.*, **OL 26**, 992–994 (2001).
8. Pogue, B. W. & Patterson, M. S. Review of tissue simulating phantoms for optical spectroscopy, imaging and dosimetry. *J Biomed Opt* **11**, 041102 (2006).
9. Feder, I., Duadi, H., Dreifuss, T. & Fixler, D. The influence of the blood vessel diameter on the full scattering profile from cylindrical tissues: experimental evidence for the shielding effect. *Journal of Biophotonics* **9**, 1001–1008 (2016).
10. Dehghani, H., Pogue, B. W., Jiang, S., Poplack, S. P. & Paulsen, K. D. Optical images from pathophysiological signals within breast tissue using three-dimensional near-infrared light. In *Optical Tomography and Spectroscopy of Tissue V* vol. 4955 191–198 (2013).
11. Dehghani, H., Pogue, B. W., Shudong, J., Brooksby, B. & Paulsen, K. D. Three-dimensional optical tomography: resolution in small-object imaging. *Appl Opt* **42**, 3117–3128 (2003).
12. Yoshimura, K. *et al.* Development of a tissue-equivalent MRI phantom using carrageenan gel. *Magnetic Resonance in Medicine* **50**, 1011–1017 (2003).
13. Hattori, K. *et al.* Development of MRI phantom equivalent to human tissues for 3.0-T MRI. *Med Phys* **40**, 032303 (2013).
14. Mano, I., Goshima, H., Nambu, M. & Iio, M. New polyvinyl alcohol gel material for MRI phantoms. *Magnetic Resonance in Medicine* **3**, 921–926 (1986).
15. Bae, K. T., Commean, P. K. & Lee, J. Volumetric measurement of renal cysts and parenchyma using MRI: phantoms and patients with polycystic kidney disease. *J Comput Assist Tomogr* **24**, 614–619 (2000).
16. Ohno, S. *et al.* Production of a human-tissue-equivalent MRI phantom: optimization of material heating. *Magn Reson Med Sci* **7**, 131–140 (2008).
17. Hellerbach, A., Schuster, V., Jansen, A. & Sommer, J. MRI Phantoms – Are There Alternatives to Agar? *PLOS ONE* **8**, e70343 (2013).
18. Kato, H. *et al.* Composition of MRI phantom equivalent to human tissues. *Med Phys* **32**, 3199–3208 (2005).
19. Shenderova, O., Hens, S. & McGuire, G. Seeding slurries based on detonation nanodiamond in DMSO. *Diamond and Related Materials* **19**, 260–267 (2010).
20. Nunn, N. & Shenderova, O. Toward a golden standard in single digit detonation nanodiamond. *physica status solidi (a)* **213**, 2138–2145 (2016).
21. Wojciechowski, A. M. *et al.* Optical Magnetometry Based on Nanodiamonds with Nitrogen-Vacancy Color Centers. *Materials* **12**, 2951 (2019).
22. Hasgall, P. A. *et al.* IT'IS Database for thermal and electromagnetic parameters of biological tissues, Version 4.0, (May 15, 2018).

23. Bazrafshan, B. *et al.* A liver-mimicking MRI phantom for thermal ablation experiments. *Med Phys* **38**, 2674–2684 (2011).
24. Brzozowski, P., Penev, K. I., Martinez, F. M., Scholl, T. J. & Mequanint, K. Gellan gum-based gels with tunable relaxation properties for MRI phantoms. *Magn Reson Imaging* **57**, 40–49 (2019).
25. Baxi, J. *et al.* Retina-simulating phantom for optical coherence tomography. *J Biomed Opt* **19**, 21106 (2014).
26. Wróbel, M. S., Popov, A. P., Bykov, A. V., Tuchin, V. V. & Jędrzejewska-Szczerska, M. Nanoparticle-free tissue-mimicking phantoms with intrinsic scattering. *Biomed. Opt. Express*, *BOE* **7**, 2088–2094 (2016).

Acknowledgements

The authors want to acknowledge the financial support of the Polish National Science Centre under Grant No. 2017/25/N/ST7/01610, the Foundation for Polish Science under the project Team-NET No. POIR.04.04.00-00-1644/1, DS Programs of Faculty of Electronics, Telecommunications and Informatics of Gdańsk University of Technology. M.S. acknowledges the scholarship in the frame of Bekker Programme PPN/BEK/2018/1/00185 funded by Polish National Agency for Academic Exchange. D.M. acknowledges the scholarship in the frame of Iwanowska Programme PPN/IWA/2018/1/00026/U/00001 funded by Polish National Agency for Academic Exchange and acknowledges K. Dholakia during her intership.

Author contributions

A.Se., D.M., R.B., A.Sa. and M.S. conceived the study and designed the experiments. A.Se., A.Sa. performed the experiments. A.Se., A.Sa., D.M., L.J. and M.S. analyzed and interpreted the data. A.Se. and M.F. prepared samples. A.S., M.K. prepared figures. A.Se., D.M., M.K., B.B.-P. and M.S. wrote the main manuscript text. All authors participated in the revision and approved the final form of the manuscript.

Competing interests

The authors declare no competing interests.

Additional information

Correspondence and requests for materials should be addressed to M.S.

Reprints and permissions information is available at www.nature.com/reprints.

Publisher's note Springer Nature remains neutral with regard to jurisdictional claims in published maps and institutional affiliations.



Open Access This article is licensed under a Creative Commons Attribution 4.0 International License, which permits use, sharing, adaptation, distribution and reproduction in any medium or format, as long as you give appropriate credit to the original author(s) and the source, provide a link to the Creative Commons license, and indicate if changes were made. The images or other third party material in this article are included in the article's Creative Commons license, unless indicated otherwise in a credit line to the material. If material is not included in the article's Creative Commons license and your intended use is not permitted by statutory regulation or exceeds the permitted use, you will need to obtain permission directly from the copyright holder. To view a copy of this license, visit <http://creativecommons.org/licenses/by/4.0/>.

© The Author(s) 2020